J. Condensed Matter Nucl. Sci. 19 (2016) 68–87

Research Article

Final Report on Calorimetry-based Excess Heat Trials using Celani Treated NiCuMn (Constantan) Wires

Arik El-Boher*, William Isaacson, Orchideh Azizi, Jinghao He, Dennis Pease and Graham Hubler

The Sidney Kimmel Institute for Nuclear Renaissance (SKINR), Department of Physics and Astronomy, University of Missouri, Columbia, MO, USA

Abstract

Sensitive mass flow calorimetry was used in a series of tests to evaluate eight treated NiCuMn (Constantan) wires in a gas loading cell. The goal of this testing was to reproduce and confirm the production of excess heat when using an experimental setup similar to that demonstrated in 2013 by Dr. Francesco Celani at National Instrument's NI week and ICCF 17. Six of the eight Constantan wires used in the SKINR tests were provided by Dr. Celani and the remaining two were obtained from Mathieu Valat. Initial tests in the series closely followed the set-up, operation, and heating protocols used by Dr. Celani with a significantly modified stainless test cell to enable the use of mass flow calorimetry. Later tests used the same modified test cell but added additional heating protocols using pulsed or highly modulated electric currents (SuperWaves) to enhance hydrogen loading and create additional thermal gradients within the Constantan wires. No excess heat was observed in a calorimeter of a sensitivity $<$10 mW when running either the initial or later test protocols during $\sim$ 200 days of testing.
 ISSN 2227-3123

Keywords: Calorimetry, Gas loading, Hydrogen, Micro-nano surface, Nickel, Nickel hydride

1. Introduction

In 2005 Baranowski and Filipek summarized 45 years of Nickel Hydride history and prospective [1]. Although palladium hydride was discovered by Graham in 1866 [2], it took almost 100 years to prove experimentally that nickel is also a hydride forming metal [3–4]. The limited penetration depth at room temperature and the fast kinetics of hydrogen desorption at normal conditions defines the Ni–H interactions [3–5]. Experiments of charging nickel of different layer thicknesses (from few micro-meters to more than 100 μm) deposited on copper wires, demonstrated that hydrogen is mainly located near the wire. These experiments showed clearly that hydrogen penetrates only about 30 μm into the bulk, below the surface [6].

*Corresponding author. E-mail: elbohera@missouri.edu

 ISSN 2227-3123

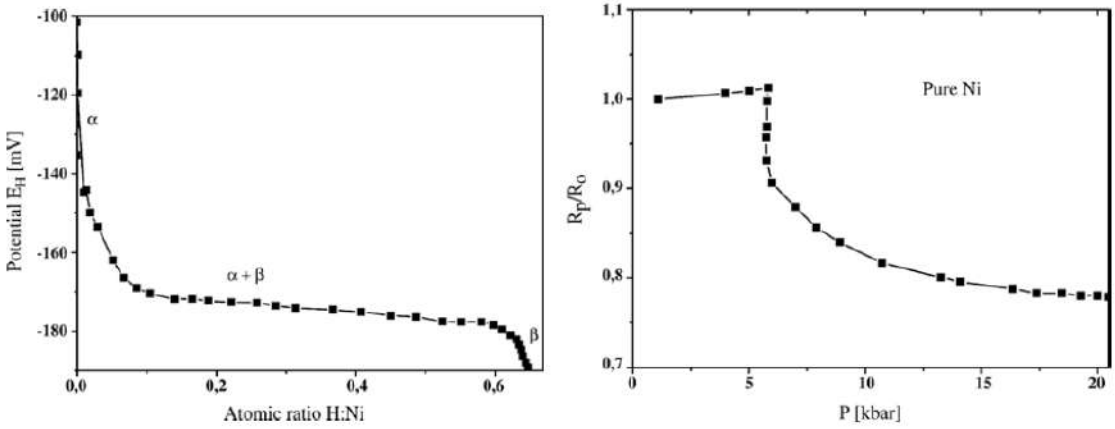

Figure 1. Data from Ref. [1].

Baranowski and Filipek [1] showed that the d-band of nickel is at least partially filled by the electrons from hydrogen during hydrogenation. Similarly, as in the Pd–H system, this filling of the d-band vacancy has radical consequences for electronic and magnetic properties of the hydride formed. For example, this results in a strong decrease of the electrical resistance, due to the reduction of the electron scattering at the d-band vacancy or/and to a decrease of the electron–phonon coupling.

On the right-hand side of Fig. 1, as shown by Baranowski [1], the relative electrical resistance ratio of a nickel sample as a function of gaseous hydrogen pressure at $25°C$ is presented. Before the hydride phase starts to form – that is below 6 kbar of gaseous hydrogen – the electrical resistance ratio rises a few percent above the initial value, due to the uptake of some hydrogen in the range of the α-phase; the dissolved hydrogen forms new scattering centers for the conduction electrons. As soon as the hydride phase is formed, the resistivity is reduced by more than 20%, becoming more metallic than in the hydrogen-free nickel. Even more radical are the changes of the magnetic properties of nickel. The ferromagnetism is lost, when going over to the hydride phase. In further electrochemical studies the electrode potential of the nickel cathode was measured as a function of the atomic ratio H/Ni of the nickel layer involved. The figure on the left presents such an example. The electrode potential measured was that of the cathode, taking the normal hydrogen electrode as reference. Clearly, three-phase regions are evident, α-phase for H/Ni atomic ratio ranging from 0 to below 0.1, the mixed $\alpha + \beta$ phase (plateau region) for H/Ni ratios up to about 0.6 and the β-phase region, in which a small change in H/Ni ratio is accompanied by steep change of electrode potential.

Starting in February 2011, Celani [7] studied the feasibility of new Nickel based alloys that are able to absorb Hydrogen (H_2) and/or Deuterium (D_2) and that have, in principle a possibility to generate anomalous heat effects at temperatures $> 100°C$.

Reports by Focardi and Piantelli [8], Miley 1996 [9] and, claims by A. Rossi and (later on) by Defkalion Company led Celani to investigate the family of NiCu alloys under high temperature H_2 gas loading. Due to theoretical considerations in a paper on catalysis (not related to LENR studies) by Romanowski et al. [10], Celani decided to explore the "large family" of CONSTANTAN alloys.

In the selection of materials, the figure of merit was the ability to decompose H_2 into H. A Constantan alloy ($Ni_{37}Cu_{63}$), among the materials studied, has the highest decomposition value (i.e. 3.2 eV); in comparison, pure Ni and Pd have values of 1.74 and 0.42 eV, respectively. Even if the alloy composition is changed to $Ni_{62}Cu_{38,}$the decomposition value remains almost constant (2.86 eV).

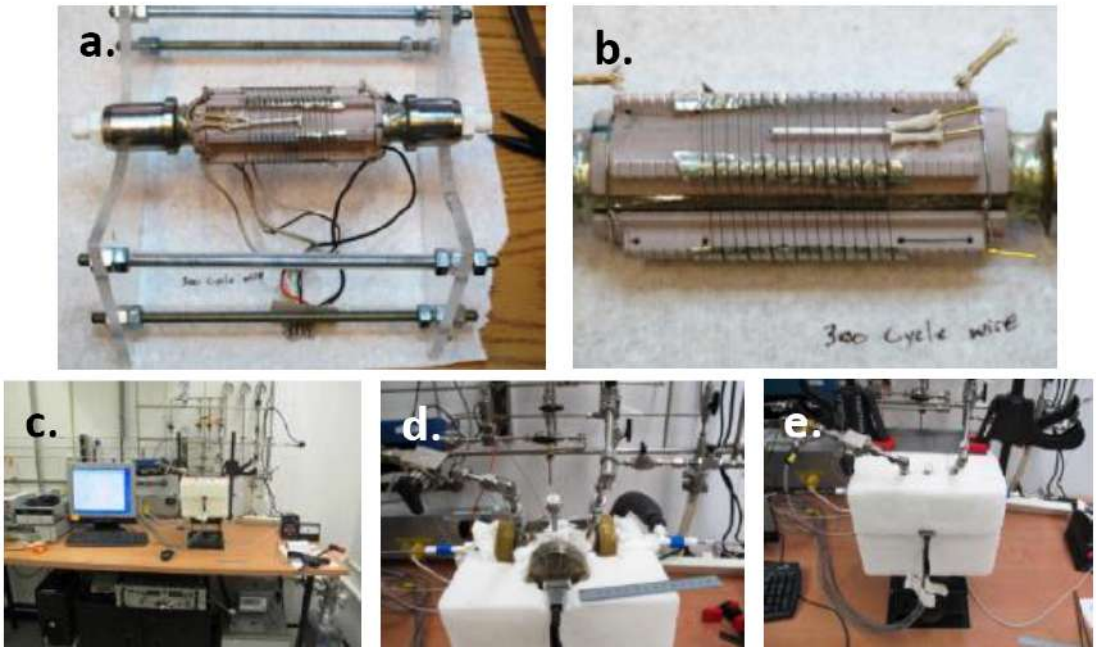

Figure 2. SKINR Test Cell.

Therefore Celani focused on a commercial (low cost) material, called ISOTAN44, with an alloy composition $Cu_{55}Ni_{44}Mn_1$, developed many years ago by Isabellenhutte Heusler, GmbH, KG-Germany. The ISOTAN 44 was selected according to the following, overall, considerations: high diffusion coefficient, low cost, good mechanical properties, high decomposition values-catalytic power (ΔE, in eV) and the ability to produce nano-micro structures on the wire's surface.

In NI week and ICCF17 Celani presented a working borosilicate Schott Duran glass cell with ISOTAN 44 wire wound on a MICA core which according to Celani's reports shows anomalous heat with a high reproducibility rate for the whole duration of the conferences. That experiment attracted the interest of SKINR which was committed to conduct an accurate calorimetric replication experiments with Celani's treated wires.

2. SKINR Test Cell and Experimental Facility

The experimental cell, as seen in Figs. 2(a)–(e) and 3, is made of a T-shaped stainless steel pressure chamber having inner diameter of 70 mm and a total length of 126 mm. Two horizontal opening of 40 mm in diameter are sealed with stainless steel flanges pressed by brass threaded nuts, against Viton O-rings. The two stainless steel flanges are supporting the inner centered ceramic (LAVA) wire holder which is riding on a stainless steel water cooled inner core. A vertical stainless steel opening is sealed with stainless steel CF multipin connector flange (Figs. 2(d) and 3). Two pins are used for measuring the ISOTAN 44 resistance when the ISOTAN wire is heated indirectly by the Nickel Chrome wire, and two pins are for delivering input electric power. In case of direct heating of the ISOTAN wire, its resistance is calculated by dividing the measured voltage by the current. Two remaining pins are for measuring the ISOTAN 44 wire temperature. All wires are connected to the pins using gold plated cylindrical 1 mm sliding

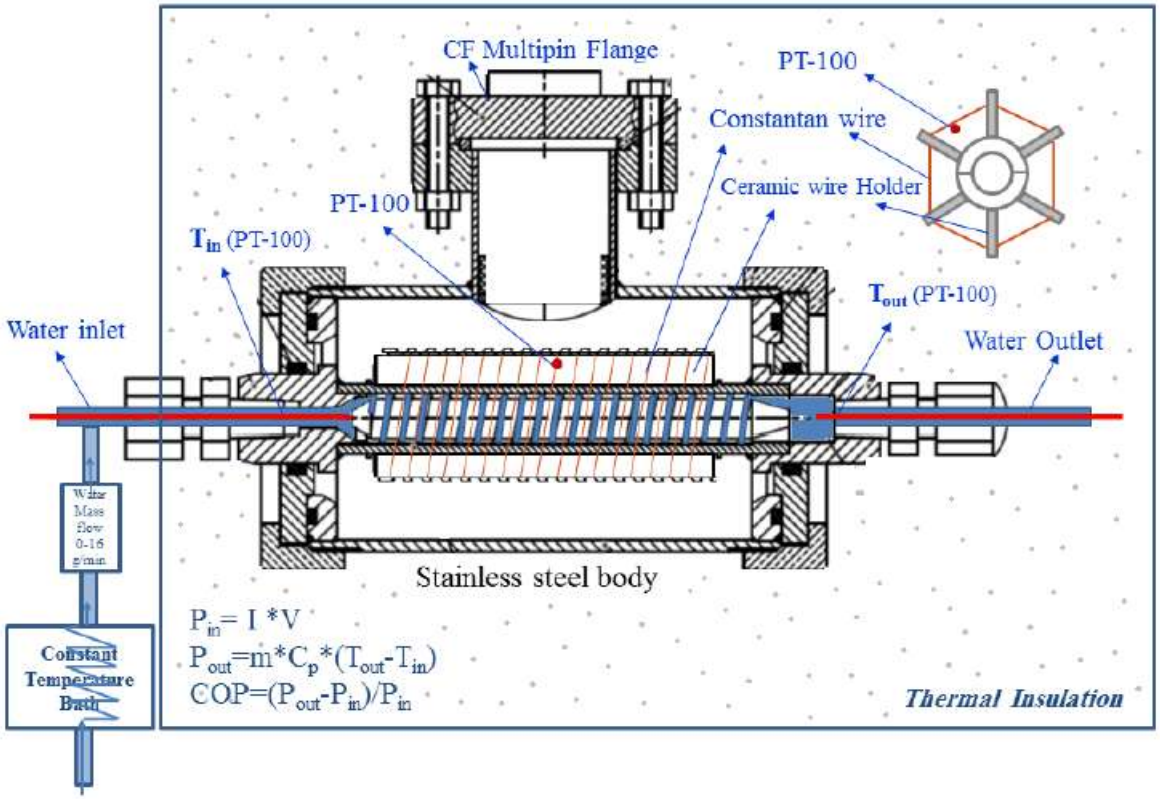

Figure 3. Experimental facility.

connectors. Cooling water flows along a spiral rectangular duct specially formed in the stainless steel core (Figs. 2(a) and 3). Heat transfers radially by convection and by radiation from the hot wires to the LAVA holder and by conduction to the stainless steel water-cooled core, which allows for accurate mass flow calorimetry. The LAVA ceramic wire's holder as seen in Fig. 2(b) has six longitudinal legs to support wires hanged freely in Hydrogen atmosphere. The legs are grooved with two nested spirals to separate the active wire from the heater wire. MICA coated glass tape are put on the face of each grooved leg to allow for further thermal barrier. The wire holder wound with treated ISOTAN 44 wire and with a 32 AWG Nickel Chrome heater wire. A PT100 RTD ceramic sheath is placed within the wires. The core assembly prior to insertion into the stainless steel chamber is shown in Fig. 2(a) and (b).

The assembled cell and the experimental facility are presented in Figs. 2(c)–(e) and 3. Figure 2(c) shows the experimental facility connected to a gas manifold containing Hydrogen, Deuterium, Argon, and Helium. Each gas can be used either separately or as a component of mixtures. Some of the experiments have been conducted with pure Hydrogen and some with Hydrogen–Argon mixture at different mixture rates to allow higher wire temperatures. The gas supply system has a mechanical pressure regulator to control the gas pressure accurately. The facility is equipped with turbine vacuum pump, so that the cell as well as the gas tubing can be evacuated down to 10^{-6} Torr before switching to a different gas or mixture, or for wire de-loading under vacuum. The cooling treated water flow rate is

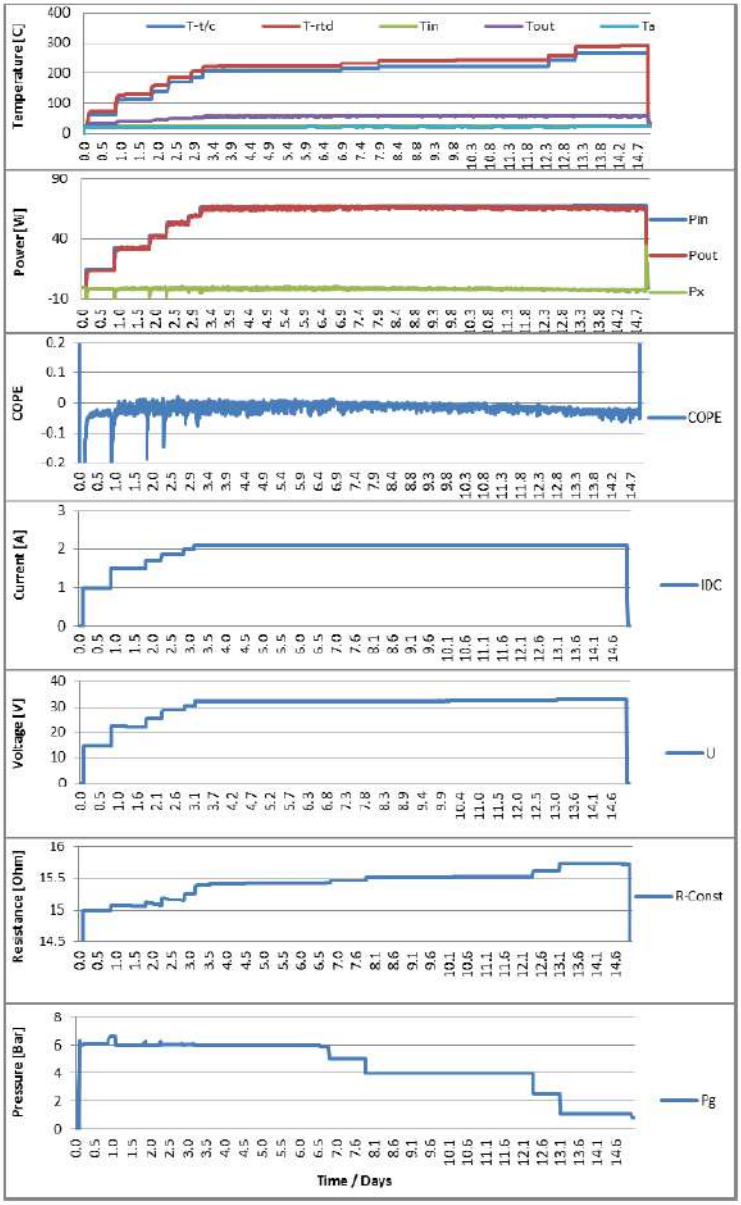

Figure 4. Wire number 270912B: 2-layer wire experiment.

controlled by a Porter Mass Flow Controller as shown in Fig. 3. Cooling water before entering the cell passes through stainless steel heat exchanger immersed in water control bath, in order to stabilize the water inlet temperature to the set point within $\pm 0.01^{\circ}$C, as shown in Fig. 3. National Instruments, in-house developed, LabVIEW data acquisition

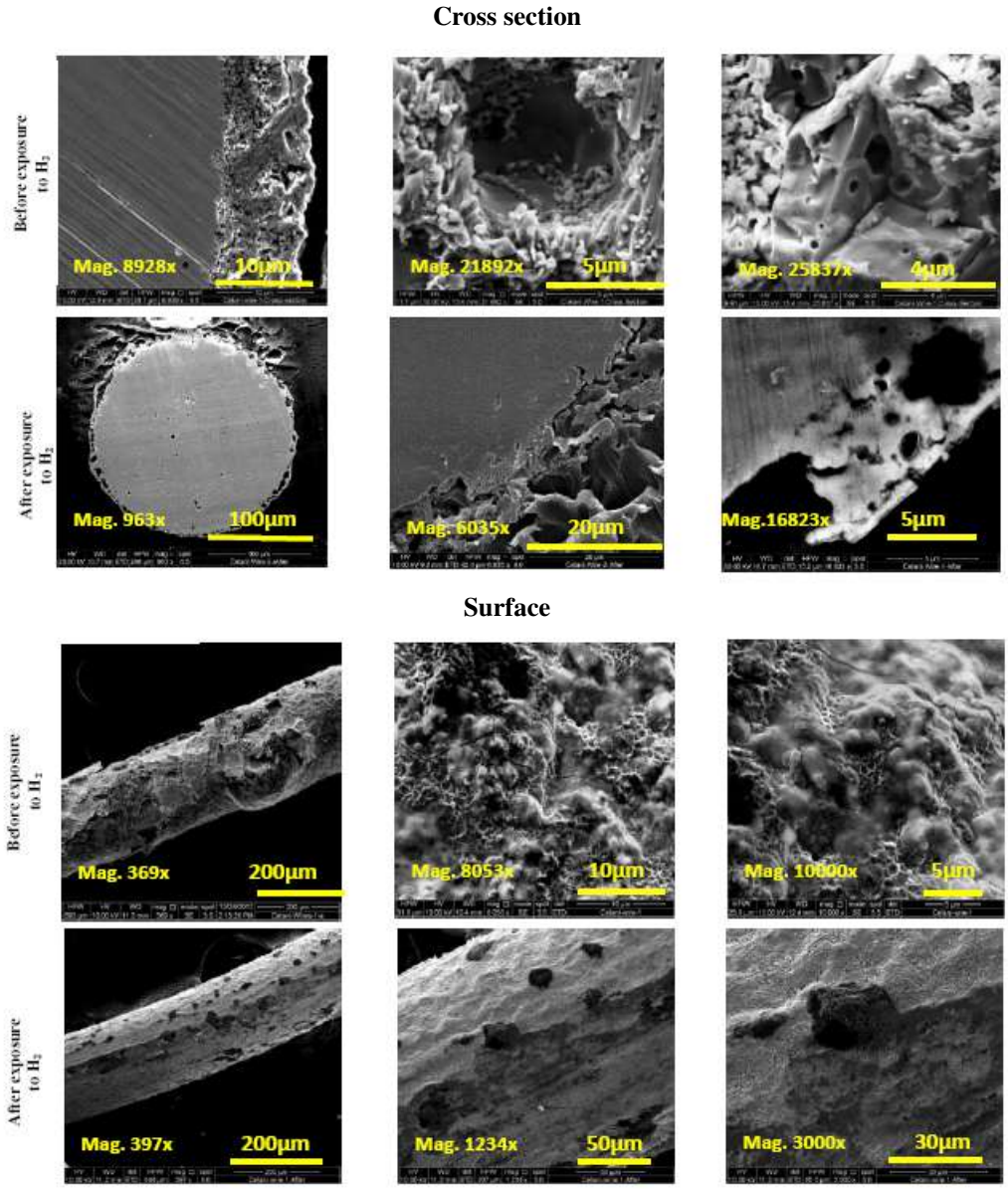

Figure 5. Cross section and surface images before and after exposure to H_2 of two layer wire.

program is used. The program allows to measure and store the cell body temperature using TC, wire, and ambient temperatures, the water inlet and outlet temperatures are measured by RTD PT-100 temperature elements. RTD PT-100 temperature elements used in experiments have an accuracy better than $\pm 0.1\%$ and with sensitivity of 0.001°C as well as the wire resistance, the water mass flow rate, the cell pressure and the electrical input parameters. The

Before exposure

Before exposure to H_2 (wire, as received)

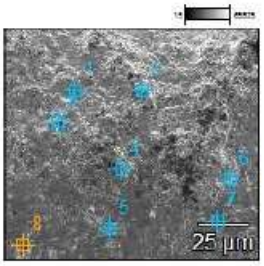

Before (wire, as received)	C-K	O-K	Si-K	S-K	Ca-K	Mn-K	Ni-L	Cu-L	W-M
Celani-1_pt1	0.59	5.35				5.23	17.96	40.87	
Celani-1_pt2	1.09	33.87	0.16			2.35	8.04	4.49	
Celani-1_pt3	4.49	33.44				1.98	8.63	1.47	
Celani-1_pt4	2.65	32.53				7.75	18.65	8.42	
Celani-1_pt5	0.54	32.63				2.45	12.89	51.49	
Celani-1_pt6	27.60	30.69	0.09	7.47	6.72		8.02	19.42	
Celani-1_pt7	0.86	31.11				2.74	10.62	54.22	0.45
Celani-1_pt8	0.41	34.71				3.72	21.10	40.06	

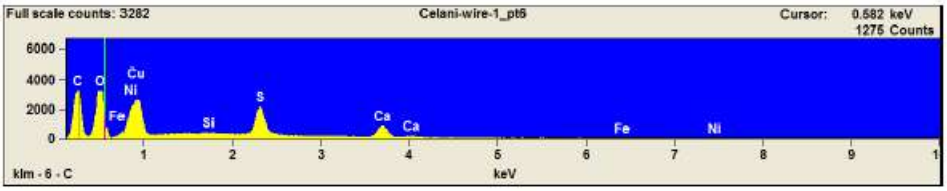

After exposure

After exposure to H_2

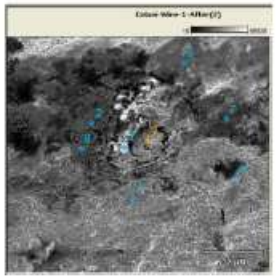

Element	Wt%	Wt% error	Atom%	Atom% error
C K	1.914	±0.21	6.91	±0.73
O K	9.46	±0.33	25.62	±0.90
Mg K	0.15	±0.06	0.26	±0.11
Si K	4.54	±0.12	7.0	±0.19
Mn K	19.42	±0.74	15.31	±0.58
Ni L	16	±2.38	11.81	±1.76
Cu L	48.52	±2.97	33.09	±2.03

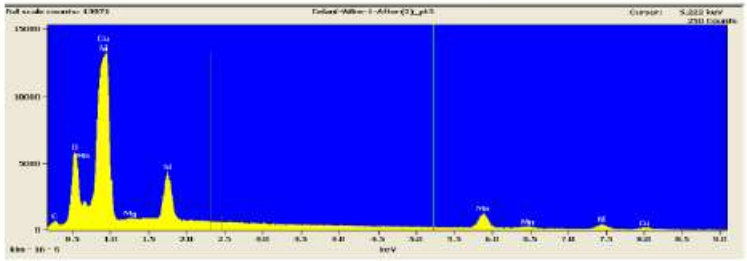

Figure 6. EDX analysis before and after exposure to H_2 of two-layer wire.

cell is energized by Kepco amplifier BOP 50-8D, which can be operated in a constant current or voltage mode. The amplifier is remotely controlled by the LabVIEW wave generator which is capable of generating DC, AC, positive and negative pulses as well as highly modulated waves (known as SuperWaves). The data acquisition system samples the temperatures, pressure and mass flow at a rate of 0.5 Hz (slow data). Simultaneously pairs of current (I) and voltage

(V) and $I \times V$ at a rate of 50 kHz are being sampled (fast data). I and V and $I \times V$ are stored on a buffer memory and then they are averaged and stored in a hard drive. Averaged input power calculated as $P_{\text{in}} = I \times V$ is compared with the output power being calculated as $P_{\text{out}} = mC_{\text{p}}(T_{\text{out}} - T_{\text{in}})$. If the difference between P_{out} and P_{in} is positive, then there is excess heat (P_x). The power gain is also calculated as COP $= (P_{\text{out}} - P_{\text{in}})/P_{\text{in}}$. Energies are calculated by integrating P_{in}, P_{out} and P_x over time and are presented as E_{in}, E_{out} and E_x. Figure 2(d) shows the assembled

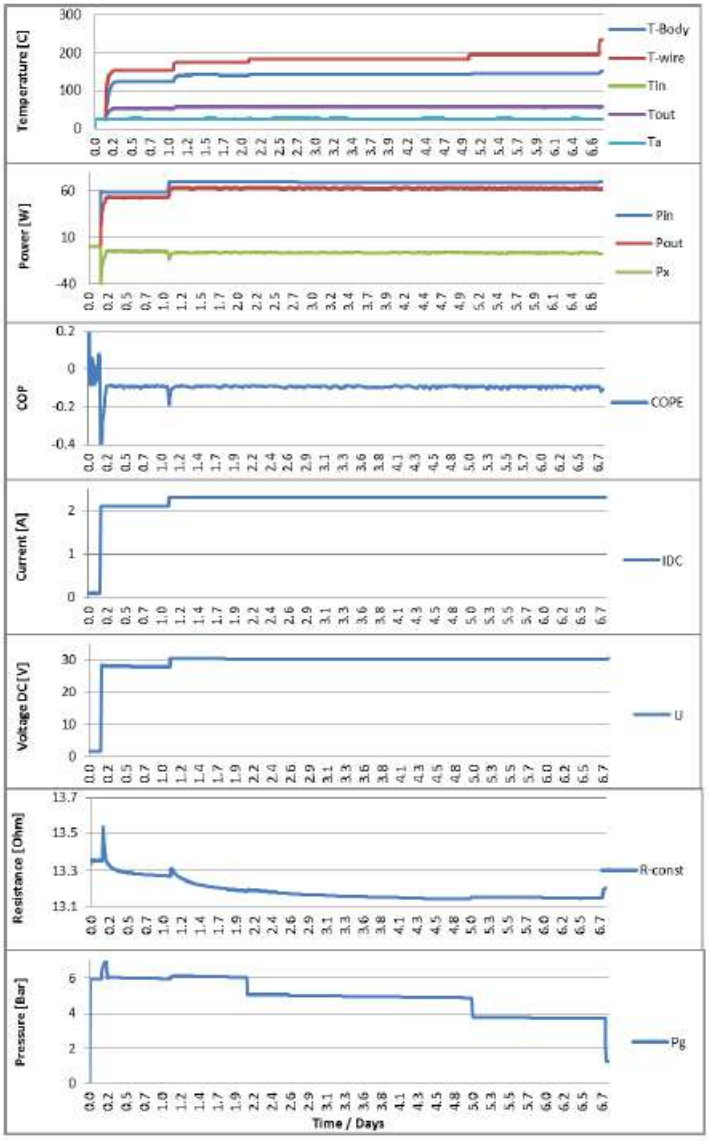

Figure 7. Wire number 280912A: 480-layer wire – initial loading.

insulated cell exposed on its upper side, in which one can identify the brass tightening nuts as well as the conflate flange with the multi-pin connector's plug. Also the gas intake/vacuum tubing and the gas vent through a needle valve can be seen. The thermally insulated cell, tubing and wiring are shown in Fig. 2(e). Figure 3 describes the water mass flow calorimeter having an accuracy of $\pm 1\%$ with sensitivity better than 10 mW. The mass flow calorimeter's

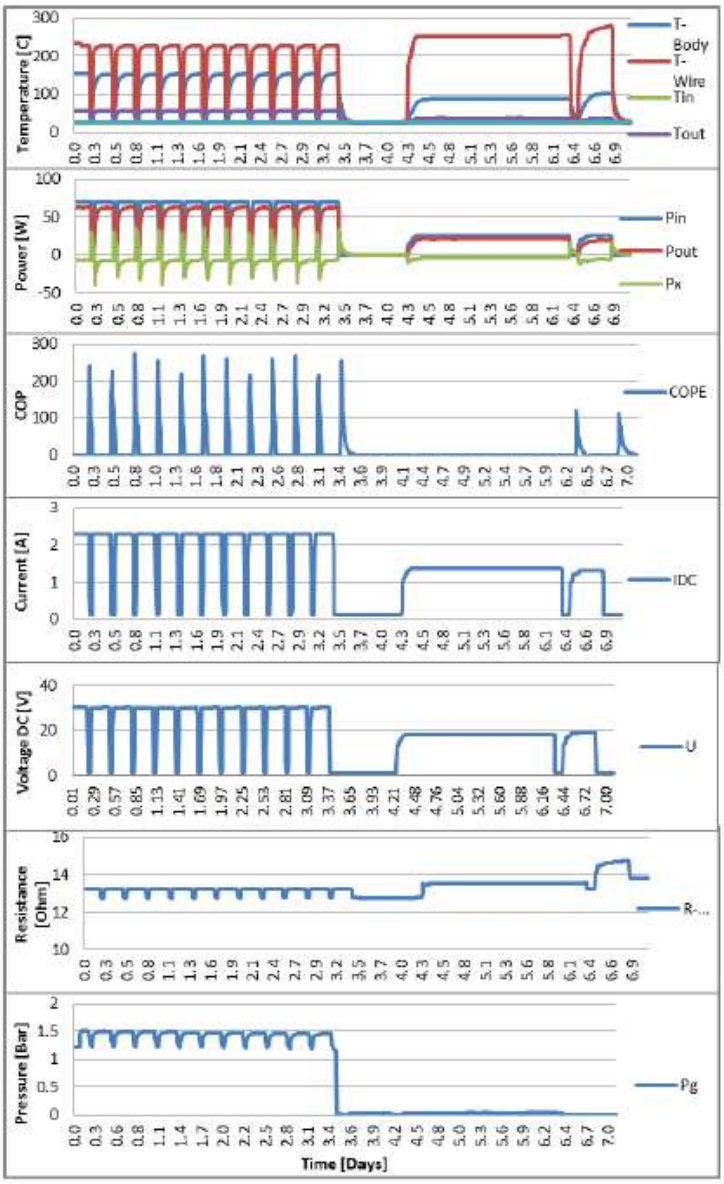

Figure 8. Pulsed power cycling – wire number 280912A: 480-layer wire 480-layer wire – initial loading.

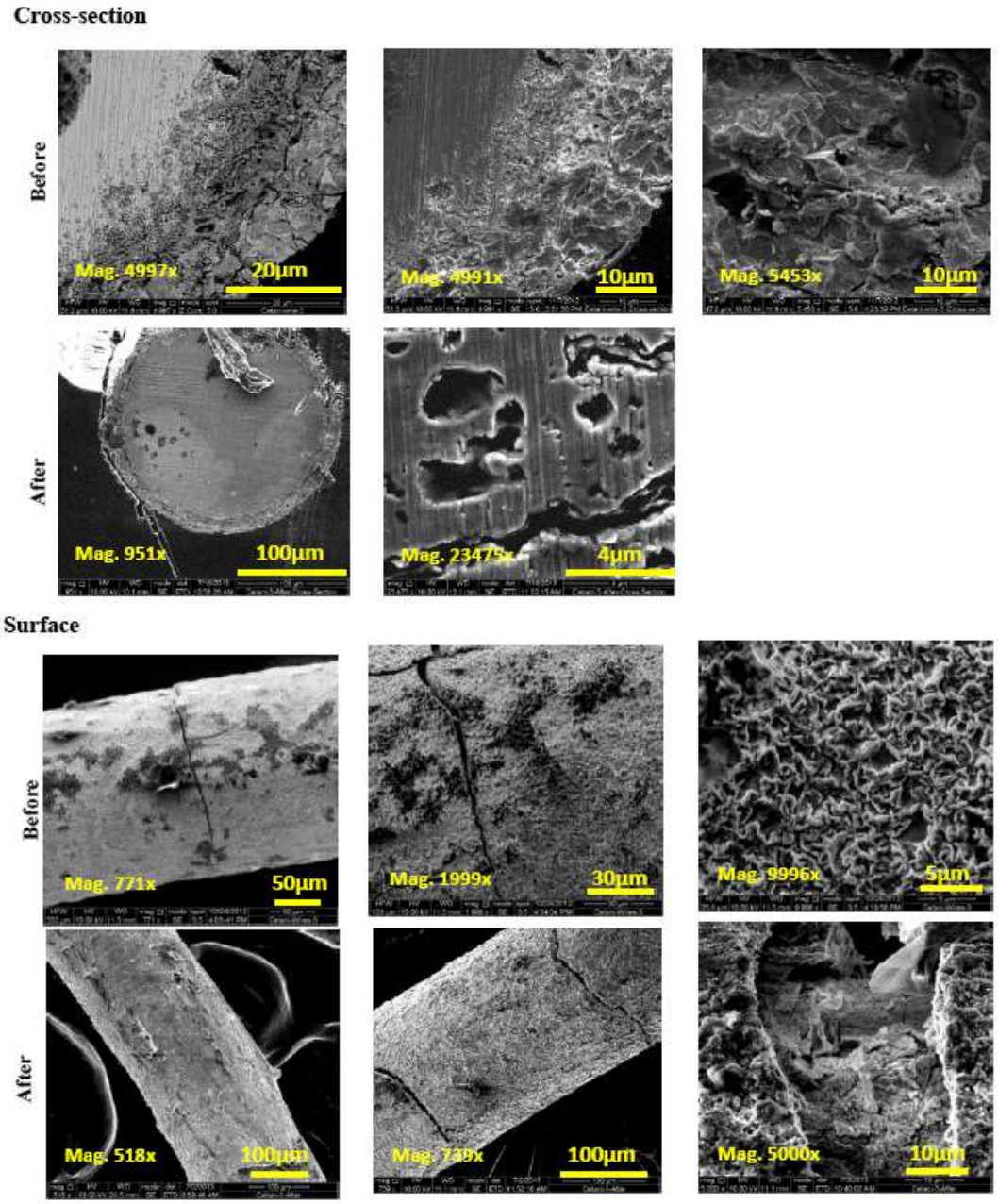

Figure 9. Cross section and surface images of 480-layer wire before and after exposure to H_2.

effectiveness varies from 95% to 90%, due to imperfect thermal insulation.

3. Results

3.1. Wire number 270912B: 2-layer wire experiment (Fig. 4)

The wire treating procedure was not disclosed to SKINR, but it is believed that the number of layers indicates the number of cycles of wire oxidation at elevated temperatures under air atmosphere.

Experiment was conducted under the following conditions: 25% Hydrogen /75% Argon atmosphere, DC current stepped to 2.1 A, electrical input power stepped up to 67 W and kept constant while gas pressure lowered in steps from 6 to 1.1 bar in order to increase the wire temperature. The initial wire resistance was 15.01 Ω. Constantan (ISOTAN 44) wire was heated indirectly by the 32 AWG Nickel Chrome wire up to a temperature of about 300°C. It can be seen from the R/R_0 vs. pressure graph in the introduction that the electrical resistance increases in α-phase and decreases after transition from α-phase to $\alpha + \beta$ and to β-phase. In this experiment a resistance increase of up to 15.7 Ω ($R/R_0 = 104\%$) was observed probably because the wire remained in α-phase region at a low hydrogen

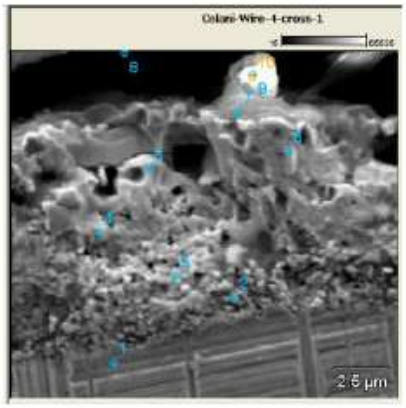

Element	Wt%	Wt% error	Atom%	Atom% error
C K	78.95	±1.46	89.47	±1.65
O K	7.61	±1.06	6.48	±0.90
Si K	0.71	±0.23	0.34	±0.11
S K	1.04	±0.21	0.44	±0.09
Cl K	2.33	±0.27	0.90	±0.10
K K	1.66	±0.29	0.58	±0.10
Ca K	1.12	±0.33	0.38	±0.11
Cu L	6.58	±0.69	1.41	±0.15

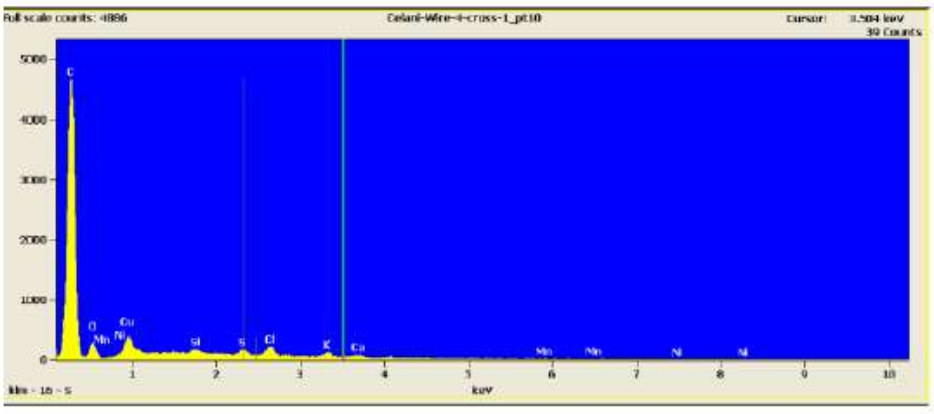

Figure 10. Cross section of 480-layer wire (number 280912A) before experiment.

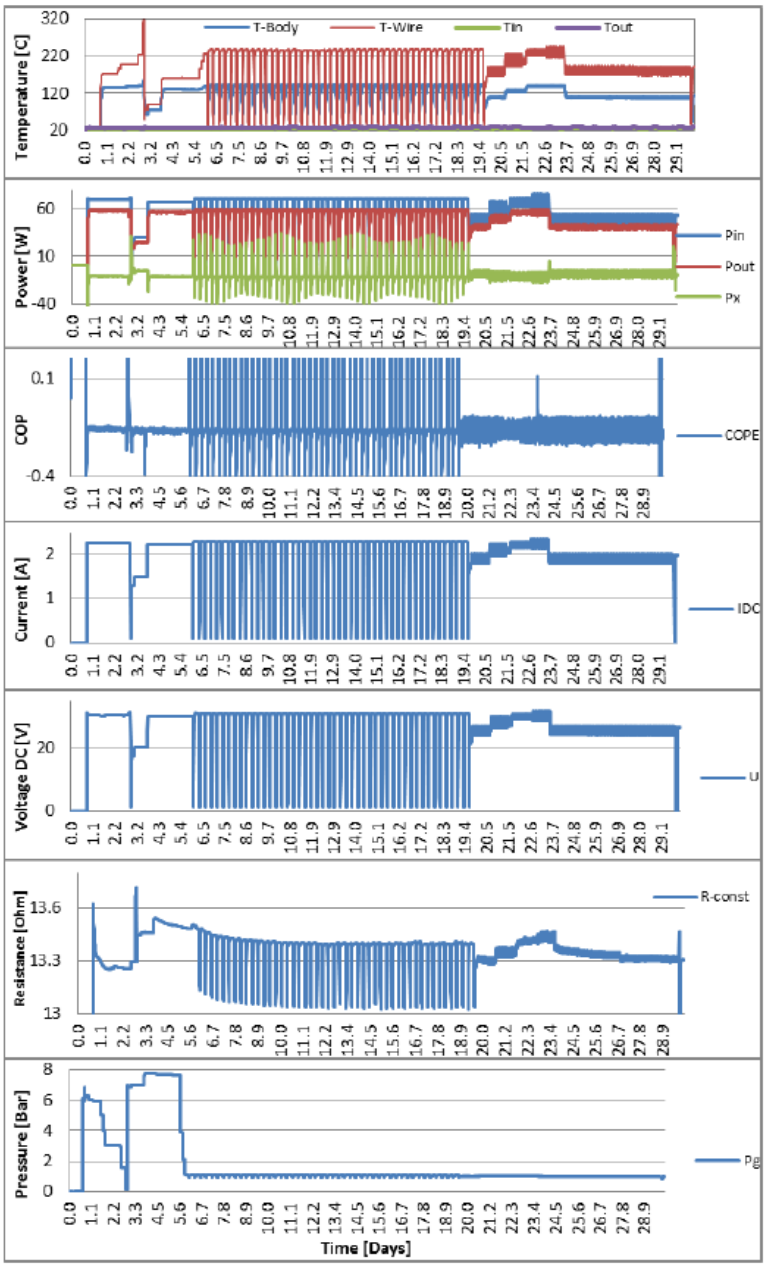

Figure 11. Pulsed power and SuperWaves cycling for the 650-layer wire (number 270912C).

loading of less than 10% H/Ni atomic ratio on average. It is believed that H/Ni ratio is higher near the surface and even higher in the nano-structures developed on the surface. No excess heat was observed ($P_{\text{out}} < P_{\text{in}}$). Experimental results with 300 L wire are similar to those with 10 L wire and therefore were not presented. The wire resistance is slightly increased, which is again an indication of relatively low loading, presumably in α-phase, which refers to atomic loading ratio (H/Ni) of less than 10%. No excess heat was observed.

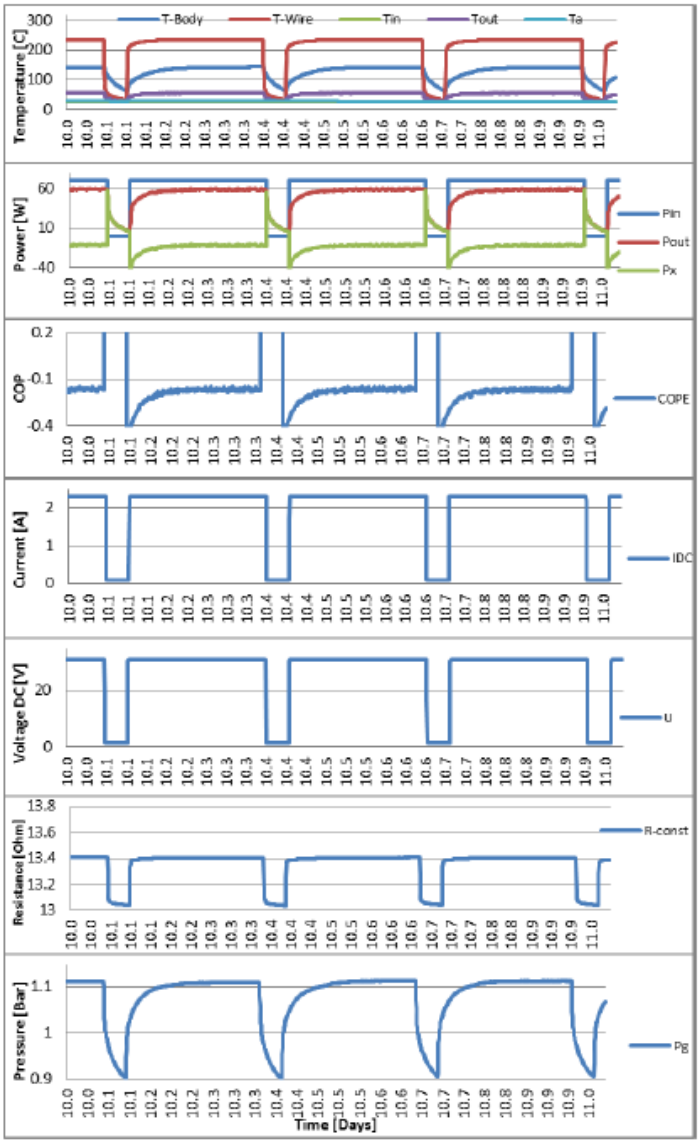

Figure 12. Pulsed power cycling for the 650-layer wire (number 270912C).

Figure 5 shows clearly that the treated wire (number $270912B$) with two layers has a higher modified surface before exposure than that after exposure to H_2. It seems that the exposed wire oxides undergo reduction in the H_2 atmosphere.

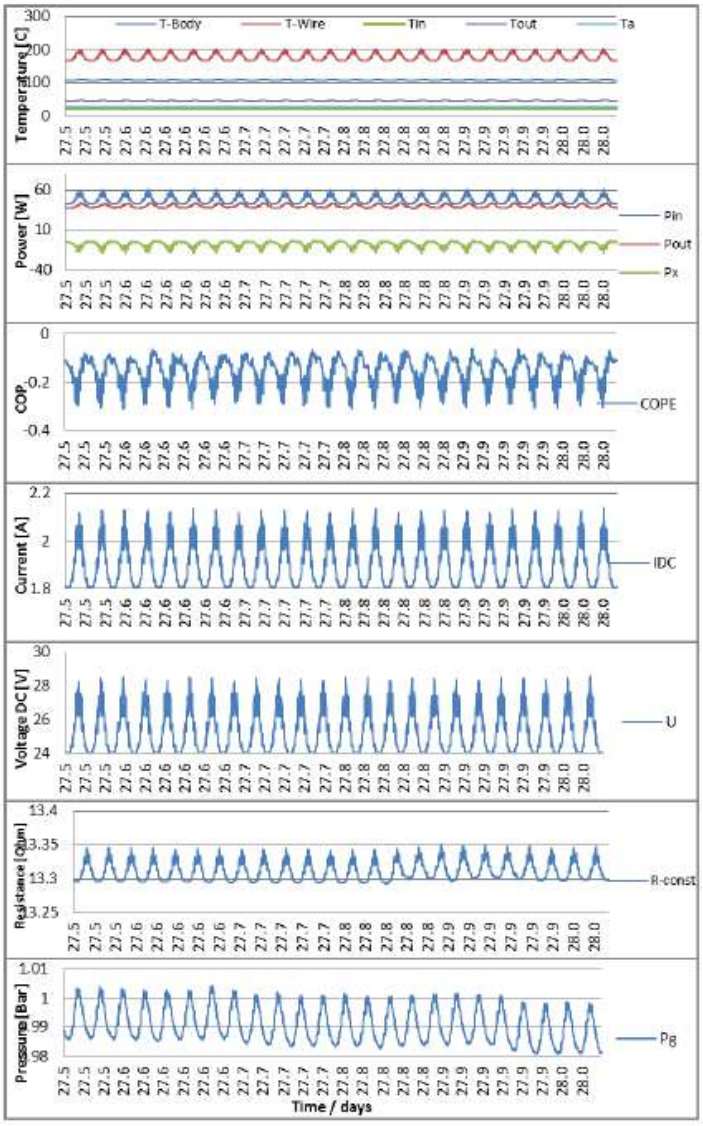

Figure 13. SuperWaves cycling for the 650-layer wire (number 270912C).

3.1.1. *The sulfur question*

Celani claimed that no excess heat achieved due to the fact that stainless steel contains 0.03% of Sulfur which is poisoning the treated wire. The stainless steel chamber was heated up to 600°C under vacuum many times prior to this set of experiments. EDX shows that the as-received ISOTAN 44 wire contains locally 7.47 wt.% Sulfur (in point 6) before exposure to H_2 as seen in the Fig.6 table; while in the other seven points analyzed, sulfur was not detected. However, no Sulfur was found after exposure to H_2 in the stainless steel chamber, suggesting that the lack of excess heat events cannot be simply explained by the use of stainless steel as confinement material although Celani used a borosilicate Schott Duran glass pipe.

3.2. Wire number 280912A: 480-layer wire – initial loading experiment (Fig. 7)

Wire running conditions are listed as follows: 100% Hydrogen atmosphere, initial wire resistance 13.37 Ω, DC current stepped up to 2.1 A and then to 2.3 A, input power stepped up to 69 W, gas pressure lowered in steps from 6 to 1.1 bar, wire temperature at 4 bar was about 200°C and at 1.1 bar was about 250°C. First run with the 480 layers wire showed that hydrogen loading was not high and electrical resistance ratio decreased to a value of about 98% ($\alpha + \beta$ phases). No excess heat was observed.

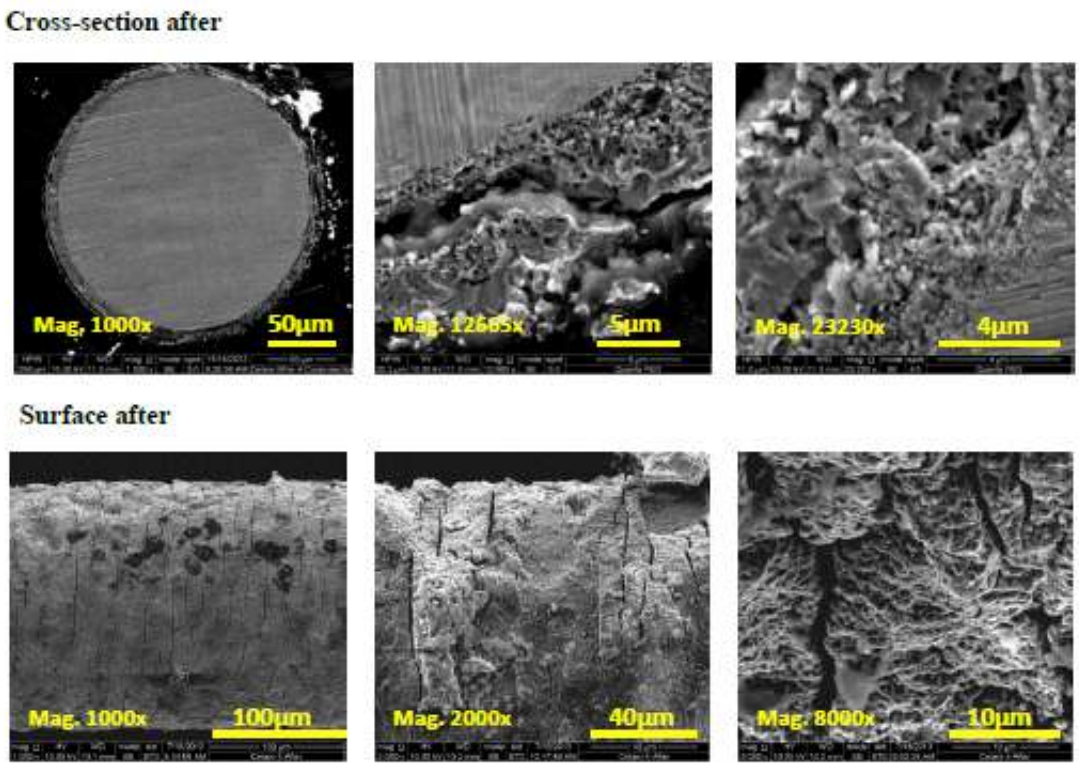

Figure 14. 650-layer wire, wire number 270912C.

3.3. Wire number 280912A: 480-layer wire – pulsed power cycling (Fig. 8)

An error in programming of input power led to an approximately 10 min disconnection between the first run (Fig. 7) and second run (Fig. 8) with the same 480 layers wire. Wire running conditions are: 100% Hydrogen atmosphere, hot cell pressure raised to 1.5 bar, pressure at room temperature was about 1.2 bar. In order to apply dynamics (excitation) to the Ni–H system, the DC current stepped up to 2.3 A for 6 h (maximum pulse input power of 69 W for 6 h) and then current reduce down to 0.1 A for 1 h. (minimum input power of 0.1 W for 1 h) Wire was de-loaded twice after the pulsed input power terminated. First de-loading was conducted under static vacuum and second under active vacuum.

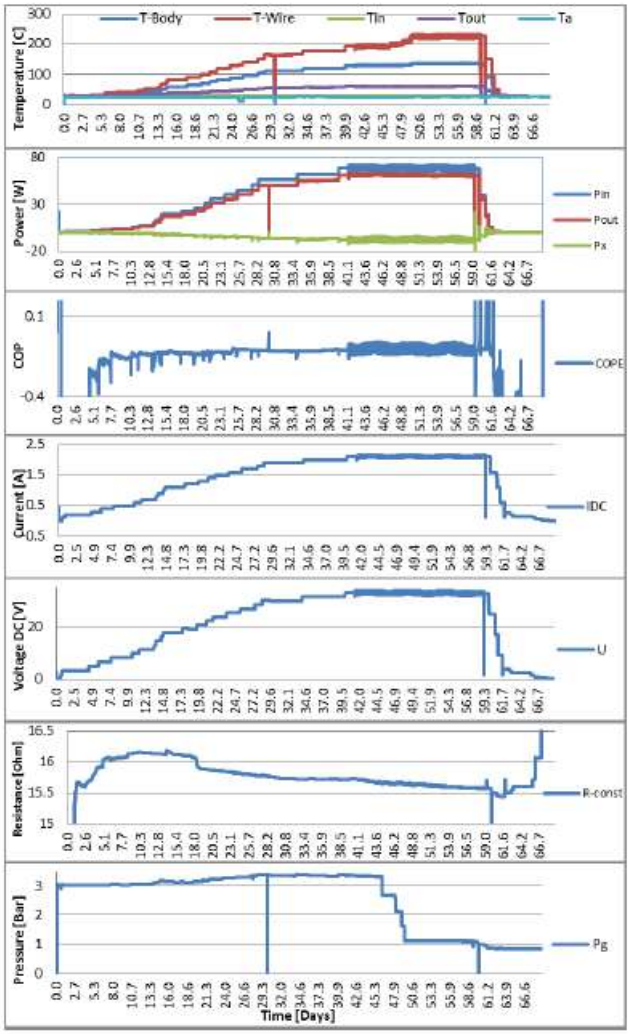

Figure 15. Cross section and surface images before and after exposure to H_2 of two layer wire.

Resistance ratio decreased to about 95%, which corresponds to low loading in $\alpha + \beta$ phase region. No excess heat was observed.

SEM images in Fig. 9 show clearly that the treated wire (number $280912A$) with 480 layers has a cracked brittle surface before exposure to H_2. It appears that after exposed to H_2 atmosphere the wire surfaces partially flaked off.

Figure 10 shows the cross section of the treated 480-layer wire before experiment where micro- and nano-structures are clearly seen. Sulfur was detected again (1.04 wt.%), on the as-received wire. The oxidized treated zone penetrates up to about 9 μm deep.

3.4. Wire number 270912C: 650-layer wire (Figs. 11–13)

Figure 11, shows the results obtained at 100% hydrogen atmosphere, DC current stepped to 2.1 A, gas pressure lowered in steps from 6 to 1.1 bar, current pulses applied with 6 h at 2.3 A (with maximum pulse input power of 71 W), followed

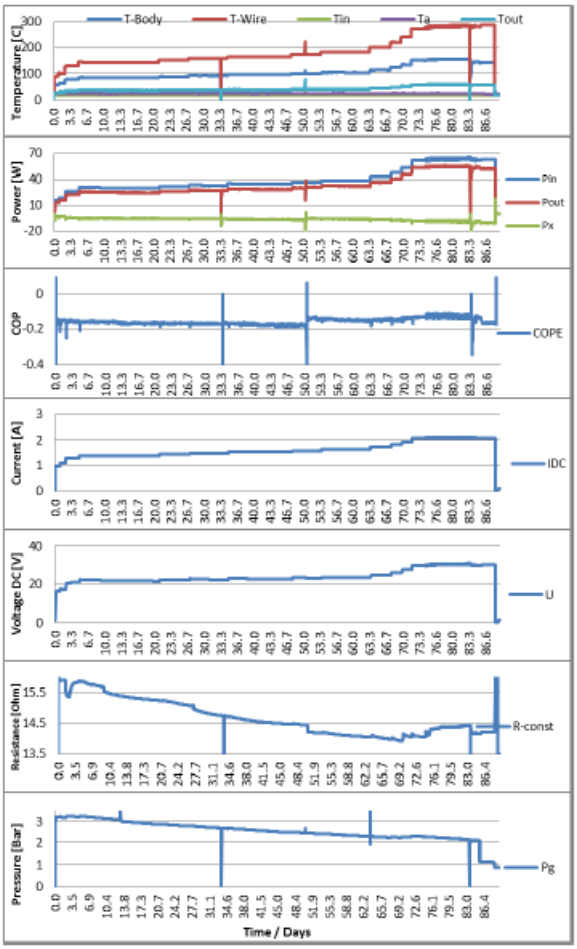

Figure 16. Cross section and surface images before and after exposure to H_2 of two layer wire.

by 1 h at 0.1 A (with minimum input power of 0.1 W). Pulses were applied for a total duration of ∼327 h, then switched to SuperWaves. After trial and error in first few waves, final wave parameters of 30 min period, 1.8 A offset, and 2.1 A average current were chosen. SuperWaves was composed of five wave modulations, with total duration of ∼243 h. Initial wire resistance was 13.67 Ω. Resistance ratio decreased to about 98%, which corresponds to low loading in $\alpha + \beta$ phase region. No excess heat was observed in DC, pulses and SuperWaves current modes. Figures 12 and 13 present a zoom in of Fig. 11 in time ranges of 10–11 days and 27.5–28 days, respectively.

In Fig. 14, the micro/nano structures due to the surface treatment can be seen with penetration depth of about 10 μm. Flakes and cracks on the surface can be seen on the surface images.

Table 1. Summary of experimental results.

Wire test no.	Treated wire	Max.R/Ro (%)	Signals used	Test duration (days)	Excess heat?	Notes:
1	2 layers #270912B	103.97	DC	15	No	
2	300 layers #021012A	103.33	DC	8	No	Wire burned through at defect
3	300 layers #021012A	101.5	DC	17	No	
4	480 layers #208912A	98.35	DC	7	No	
5	480 layers #208912A	95.32	DC and Pulsed DC	7	No	
6	650 layers #270912C	97.69	DC, Pulsed DC and SW	20	No	Performed with Dr. Celani in attendance
7	10 layers #020813	95.70	DC and SW	69	No	Lot-2 wire received from Dr. Matthew Valat
8	200 layers #050813	87.00	DC and SW	90	No	Lot-2 wire received from Dr. Matthew Valat

In Fig. 14, the micro/nano structures due to the surface treatment can be seen with penetration depth of about 10 μm. Flakes and cracks on the surface can be seen on the surface images.

3.5. Wire number 020813: 10-layer wire (Fig. 15)

This wire is from a second lot provided by Dr. Matthew Valat. The experiment was conducted at the conditions of 100% hydrogen atmosphere, DC current stepped up to 2.1 A, followed by current SuperWaves with 2.1 A average, the input power at maximum was 68 W and gas pressure lowered in steps from 3 to 1.1 bar. The initial wire resistance was 15.01 Ω. Resistance ratio reduced to 95.7%. No excess heat was observed in this experiment.

3.6. Wire number 050813: 200-layer wire (Fig. 16)

This wire is again from a second lot provided by Dr. Matthew Valat. The experiment of hydrogen loading in this wire was conducted under the same conditions as the 10-layer wire (number 020813). The initial wire resistance was 16.10 Ω and it dropped by about 13% (R/R_0= 0.87), due to hydrogen loading. The loading ratio was higher than in previous experiments and is clearly in the mixed $\alpha + \beta$ phase with H/Ni ratios less than 0.6. In spite the fact that the resistance ratio is in the same range as achieved in Dr. Celani's experiments (0.9–0.8), no excess heat was observed. Under similar R/R_0, Dr. Celani reported the observation of 10–20 W excess heat with an input power of 48 W.

4. Conclusions

In short, we list all experimental results in Table 1 showing wire numbers, maximum measured hydrogen resistance ratios, applied power modes, and test durations. We conclude our tests as follows.

- Dr. Celani's wire preparation process appears to be a selective oxidation/reduction of the Nickel/Copper/Manganese wire.
- The number of layers equates to the number of pulsed oxidation cycles that the wire has been put through and correlates with the thickness of the treated surface and with the micro-nano surface morphology.
- Obtaining an accurate temperature reading of such a small wire is problematic, actual temperature is higher.
- Loading studies in pure nickel have been done by Baranowski and Filipek. Unfortunately calibration curves of R/R_0 vs. H/Ni atomic ratio, for pure nickel and definitely for Constantan are not available, as are available for H/Pd and for D/Pd. This tool is essential for understanding the mechanism of excess heat. Further studies on gas loading in Ni systems are most important, especially due to researchers (Rossi, Parkhomov, and others) which are reporting on positive results in Ni/H systems. Furthermore, when the wire reaches certain temperatures, there is a reduction of the Nickel oxides which affects the wire resistance.
- Loading as indicated by resistance and by pressure reduction was much better for the second lot of wires.
- In seven out of eight runs conducted in SKINR's replication study, using wires treated by Celani and applying Celani's running protocol, R/R_0 values achieved were higher than 92%, which corresponds to low loading ratios of less than 10% atomic ratio. Celani is reporting in his experiments, on R/R_0 values of 92–80%, followed by excess heat. It is most probable that in the first seven experiments, no excess heat was observed, maybe due to low hydrogen loading. High loadings (atomic ratios) are accepted as a necessary condition, in Pd/D systems, for increasing the probability to achieve excess heat.
- Only in the last Experiment #050813 with 200 layers wire, the resistance ratio achieved was in within the range Dr. Celani obtained, but no excess heat was observed. At this level of loading Dr. Celani showed excess heat. It is most recommended that Dr. Celani will conduct future experiments with mass flow calorimetry.

Acknowledgment

This work is fully supported by Mr. Sidney Kimmel.

References

[1] B. Baranowski and S.M. Filipek, *J. Alloys Compounds* **404–406** (2005) 2–6.
[2] T. Graham, Philos. *Trans. Roy. Soc.* **156** (1866) 415.
[3] B. Baranowski and M. Smiaşowski, *Bull. Polon. Acad. Sci.* 7 (1959) 663.
[4] B. Baranowski and M. Smiaşowski, *J. Phys. Chem. Solids* **12** (1959) 206.
[5] A. Stroka and B. Baranowski, *Pol. J. Chem.* **76** (2002) 1019.

[6] B. Baranowski, Z. Szklarska-Smiaşowska and M. Smiaşowski, *Bull. Polon. Acad. Sci.* **6** (1958) 179.
[7] F. Cellani, E.F Marano, A. Spallone, A. Nuvoli, E. Purchi, M. Nakamura, B. Ortenzi, S. Pella, E. Righi, G. Trenta, S. Bartalucci, G.L. Zangari, F. Micciulla and S. Bellucci, Cu—Ni–Mn alloy wires, with improved sub-micrometric surfaces, used as LENR device by new transparent, dissipation-type, calorimeter, in *Proc 17th Int. Conf. on Condensed Matter Nuclear Science* (*ICCF 17*), South Korea, Daegeon, 2012.
[8] S. Focardi, V. Gabbani, V. Montalbano, F. Piantelli and S. Veronesi, Asti Workshop on Hydrogen/Deuterium loaded metals, *Conf. Proc. 64*, W.J.M.F. Collis editor, 1999, p. 35.
[9] G.H. Miley and J.A. Patterson, *J. New Energy* **1** (1996) 5.
[10] S. Romanowski, W. M. Bartczak and R. Wesoşkowski, *Langmuir* **15** (1999) 5773.